Title
Basal crevasses on the Larsen C Ice Shelf, Antarctica: Implications for meltwater ponding and hydrofracture

Journal
Geophysical Research Letters, 39(16)

ISSN
0094-8276

Authors
McGrath, Daniel
Steffen, Konrad
Rajaram, Harihar
et al.

Publication Date
2012-08-28

DOI
10.1029/2012gl052413

Basal crevasses on the Larsen C Ice Shelf, Antarctica: Implications for meltwater ponding and hydrofracture

Daniel McGrath,[1] Konrad Steffen,[1] Harihar Rajaram,[2] Ted Scambos,[3] Waleed Abdalati,[1,4] and Eric Rignot[5,6]

Received 1 June 2012; revised 20 July 2012; accepted 23 July 2012; published 29 August 2012.

[1] A key mechanism for the rapid collapse of both the Larsen A and B Ice Shelves was meltwater-driven crevasse propagation. Basal crevasses, large-scale structural features within ice shelves, may have contributed to this mechanism in three important ways: i) the shelf surface deforms due to modified buoyancy and gravitational forces above the basal crevasse, creating >10 m deep compressional surface depressions where meltwater can collect, ii) bending stresses from the modified shape drive surface crevassing, with crevasses reaching 40 m in width, on the flanks of the basal-crevasse-induced trough and iii) the ice thickness is substantially reduced, thereby minimizing the propagation distance before a full-thickness rift is created. We examine a basal crevasse (4.5 km in length, ∼230 m in height), and the corresponding surface features, in the Cabinet Inlet sector of the Larsen C Ice Shelf using a combination of high-resolution (0.5 m) satellite imagery, kinematic GPS and in situ ground penetrating radar. We discuss how basal crevasses may have contributed to the breakup of the Larsen B Ice Shelf by directly controlling the location of meltwater ponding and highlight the presence of similar features on the Amery and Getz Ice Shelves with high-resolution imagery. **Citation:** McGrath, D., K. Steffen, H. Rajaram, T. Scambos, W. Abdalati, and E. Rignot (2012), Basal crevasses on the Larsen C Ice Shelf, Antarctica: Implications for meltwater ponding and hydrofracture, *Geophys. Res. Lett.*, *39*, L16504, doi:10.1029/2012GL052413.

1. Introduction

[2] A key mechanism for the rapid and catastrophic collapse of both the Larsen A and B Ice Shelves was meltwater-driven crevasse propagation [*Rott et al.*, 1996; *Scambos et al.*, 2000, 2003, 2009]. This mechanism contends that when sufficient ponded meltwater drains into a surface crevasse, the crevasse will propagate through the entire ice shelf thickness (due to the density difference between water and ice), fracturing the ice shelf into numerous elongate icebergs [*van der Veen*, 1998, 2007; *Scambos et al.*, 2003, 2009; *Weertman*, 1973]. The narrow along-flow width and elongated across-flow length of these icebergs distinguishes them from tabular icebergs, and likely facilitates a positive feedback during the disintegration process, as elongate icebergs overturn and initiate further ice shelf calving [*MacAyeal et al.*, 2003; *Guttenberg et al.*, 2011; *Burton et al.*, 2012].

[3] Dramatic atmospheric warming over the past five decades has increased surface meltwater production along the Antarctic Peninsula (AP) [*Vaughan et al.*, 2003; *van den Broeke*, 2005; *Vaughan*, 2006]. As the summer air temperature of large portions of the AP hovers near 0°C, the AP is sensitive to even a modest warming, unlike the interior regions of Antarctica [*Vaughan*, 2006]. While the final disintegration of Larsen A and B has been attributed to meltwater-driven crevasse propagation, numerous processes pre-condition an ice shelf for rapid collapse [*Doake et al.*, 1998; *Vieli et al.*, 2007; *Khazendar et al.*, 2007; *Glasser and Scambos*, 2008]. Firn densification and melt layer formation allow surface melt ponds to form on the shelf surface, a process that can take multiple melt seasons to accomplish [*Scambos et al.*, 2000, 2003]. Concurrently, increased basal submarine melting or reduced marine ice accretion can thin an ice shelf and reduce the cohesion between parallel flow bands and / or shear margins [*Glasser and Scambos*, 2008; *Jansen et al.*, 2010]. This may lead to ice flow acceleration, with increased crevassing and rifting due to elevated strain rates, as observed on Larsen B prior to its collapse [*Rignot et al.*, 2004]. Increased calving and subsequent frontal retreat is also a clear harbinger of ice shelf disintegration, particularly if the ice front retreats past a critical compressive arch in the strain field, at which point substantial retreat will occur before reaching a new stable configuration [*Doake et al.*, 1998].

[4] Larsen C is the largest remaining ice shelf on the AP, consisting of over 50,000 km^2 of floating ice, which is fed from 12 major outlet glaciers (Figure 1a) [*Glasser et al.*, 2009; *Cook and Vaughan*, 2010]. The extent of Larsen C has been relatively stable over the last five decades, outside of calving events in 1986 and 2004/05 where the ice shelf lost ∼7700 km^2 and ∼1500 km^2, respectively [*Glasser et al.*, 2009; *Cook and Vaughan*, 2010]. Despite limited changes in extent, the surface elevation of Larsen C has lowered at a rate of between 0.06 and 0.09 m a^{-1} during the 1978–2008 period, with the greatest lowering occurring in the northern sector [*Fricker and Padman*, 2012; *Shepherd et al.*, 2003]. This surface lowering is likely dominated by firn densification driven by warmer air temperatures and increased meltwater production / refreezing [*Holland et al.*, 2011; *Fricker and Padman*, 2012] rather than increased basal melting

[1]Cooperative Institute for Research in Environmental Sciences, University of Colorado Boulder, Boulder, Colorado, USA.
[2]Department of Civil Engineering, University of Colorado Boulder, Boulder, Colorado, USA.
[3]National Snow and Ice Data Center/CIRES, University of Colorado Boulder, Boulder, Colorado, USA.
[4]NASA Headquarters, Washington D.C., USA.
[5]Department of Earth System Science, University of California, Irvine, California, USA.
[6]Jet Propulsion Laboratory, California Institute of Technology, Pasadena, California, USA.

Corresponding author: D. McGrath, Cooperative Institute for Research in Environmental Sciences, University of Colorado Boulder, Boulder, CO 80309, USA. (daniel.mcgrath@colorado.edu)

0094-8276/12/2012GL052413

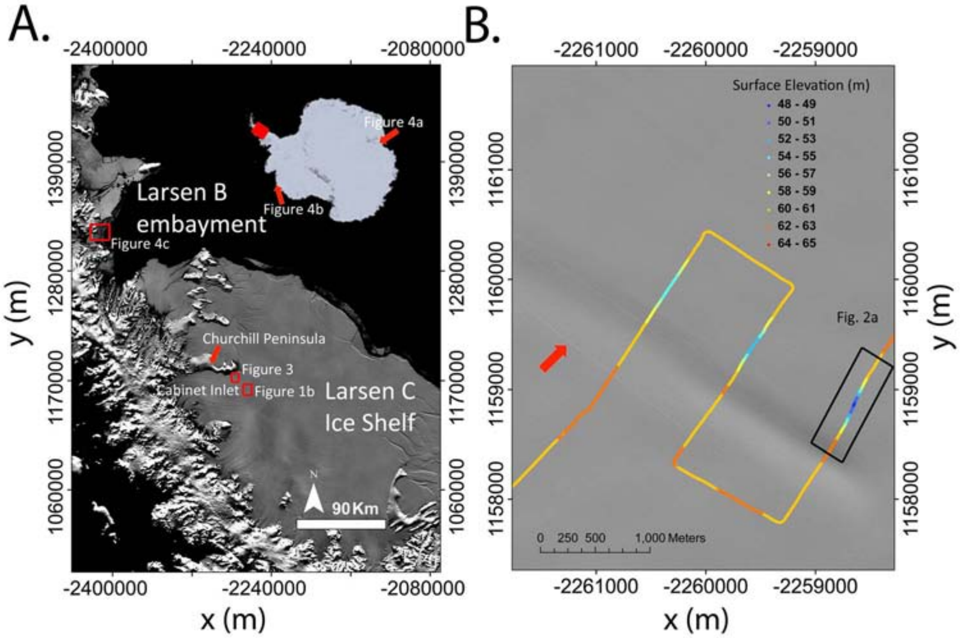

Figure 1. (a) Subsection of MODIS MOA mosaic detailing the Larsen C Ice Shelf [*Haran et al.*, 2005]. White boxes indicate location of Figure 1b and red arrows on inset indicate location of Figure 4. Coordinates are polar stereographic (at 71°S secant plane, 0° meridian) where x is easting and y is northing. (b) High-resolution (0.5 m) visible imagery of surface depressions and surface crevasses, located on flanks of the depressions. Surface elevations from kinematic GPS are shown as colored transect. Black box indicates location of radar profile shown in Figure 2a. Red arrow is aligned with flow direction and identifies bridged surface crevasses. Note spatial offset between depression in kinematic GPS data and visual imagery due to temporal offset between image and GPS collection. Imagery Copyright GeoEye Inc., 2011.

driven by an ocean forcing [*Shepherd et al.*, 2003]. Oceanographic observations suggest that the primary water mass in the Larsen C cavity is Modified Weddell Deep Water, which has been cooled to the surface freezing point, and is thus not likely to drive high basal melt rates [*Nicholls et al.*, 2004]. *Khazendar et al.* [2011] found that the northern sector of the ice shelf accelerated by 80 m a^{-1} or 15% between 2000 and 2006, and a further 6–8% between 2006–2008 in the vicinity of Cabinet Inlet, possibly due to a reduction in backstress from the Bawden Ice Rise and/or the erosion of marine ice formerly suturing parallel flow bands together.

[5] Airborne radar surveys, beginning in the late 1970's, identified large hyperbolic radar returns, interpreted as basal crevasses, within the Ross [*Jezek et al.*, 1979; *Shabtaie and Bentley*, 1982], Larsen [*Swithinbank*, 1977], and the Riiser-Larsen Ice Shelves [*Orheim*, 1982]. Despite the magnitude and abundance of these features, they have received relatively little attention, especially in light of recent ice shelf disintegrations. Recent work by *Bindschadler et al.* [2011], *Humbert and Steinhage* [2011], *Luckman et al.* [2012], and *McGrath et al.* [2012] has identified numerous basal crevasses, and their corresponding surface expressions, on the Pine Island Glacier, Fimbul and Larsen C Ice Shelves. Basal crevasses in two different regions on Larsen C penetrate between 69 and 217 m into the overlying ice shelf, representing between ~24 and 66% of the ice thickness and likely have basal opening widths ranging from tens to hundreds of meters [*Luckman et al.*, 2012; *McGrath et al.*, 2012]. In addition to representing structural weaknesses in the ice shelf, basal crevasses also modulate the exchange of mass and energy between the ice shelf and ocean by increasing both the ice-ocean interface area [*Luckman et al.*, 2012] and the basal surface roughness. It is difficult to speculate the net basal melting or accretion due to the presence of basal crevasses, as these processes are dependent on unknown ocean properties and circulation in close proximity to the basal crevasses.

2. Methods

[6] Analysis of the surface depressions and crevasses was conducted using a subset of the MODIS Mosaic of Antarctica [*Haran et al.*, 2005] (125 m resolution), Landsat 7 ETM+ imagery (Band 8; 15 m resolution; collected 15 December 2001), a GeoEye-1 panchromatic image (0.5 m resolution; collected 25 February 2010) and WorldView-1 panchromatic imagery (0.5 m; collected 24 November 2008 and 18 October 2009). Radar surveys (Figures 2a and 3b) were conducted with a Malå Geosciences ground based pulse radar system with a 25 MHz antenna towed behind a snowmobile. The in situ data, including kinematic GPS, were collected in November 2011, and therefore a temporal (and hence spatial) offset exists between the in situ data and the imagery (Figures 1b and 3a). Following previous studies [*Luckman et al.*, 2012; *McGrath et al.*, 2012], the measured two-way travel time was converted to depth assuming a mean radar velocity of 0.173 m ns^{-1}. The ice shelf-ocean interface reflection was manually delineated along the profile by following the maximum echo amplitude in the radar waveform. Uncertainty in the derived ice thickness is assumed to be ±5% due to uncertainty in radar velocity and resolution of radar wavelength. Simultaneous position data were collected

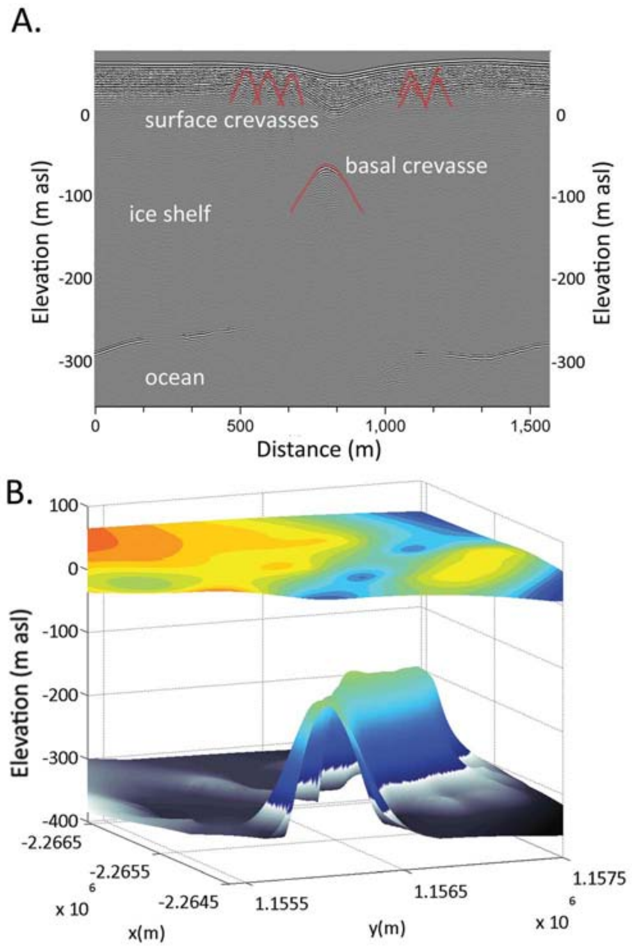

Figure 2. (a) 25 MHz radar profile across basal and surface crevasses. Surface elevations have been corrected to reflect ice shelf topography. Note down warping of firn above basal crevasse and hyperbolas on the flanks, highlighted in red, interpreted as surface crevasses. (b) Three-dimensional view of the basal crevasse penetrating into the ice shelf. Surface and basal interface interpolated from GPS and GPR profiles, respectively.

with a dual-frequency GPS and corrected to the Eigen GL04C ellipsoid [*Förste et al.*, 2008] and further corrected for tidal amplitude using Circum-Antarctic Tidal Simulation version 2008a (CATS2008a), updated from *Padman et al.* [2002].

3. Results and Discussion

[7] Visible imagery details a series of isolated surface depressions in the main outflow of Cabinet Inlet, extending seaward to the calving front (Figure 1a). We focus our observations on one of these features (Figure 1b). The surface depression has a maximum depth of 13.0 m and extends for 4.5 km, as measured from kinematic GPS and imagery, respectively (Figure 1b). A large hyperbolic reflection within the ice column is aligned with the surface depression, which we interpret as the apex of a basal crevasse (Figure 2a). It extends 233 ± 11 m in height from the base of the ice shelf, penetrating through over 66% of the mean local ice thickness and is 470 m in width (Figures 2a and 2b). The size of the basal crevasse increases the local ice-ocean interface by ~30% relative to a flat-bottomed ice shelf. Above the hyperbolic reflection, the firn and upper ice layers down warp by 15–20 m (Figure 2a). Numerous snow-bridged surface crevasses, with widths between 20–25 m,

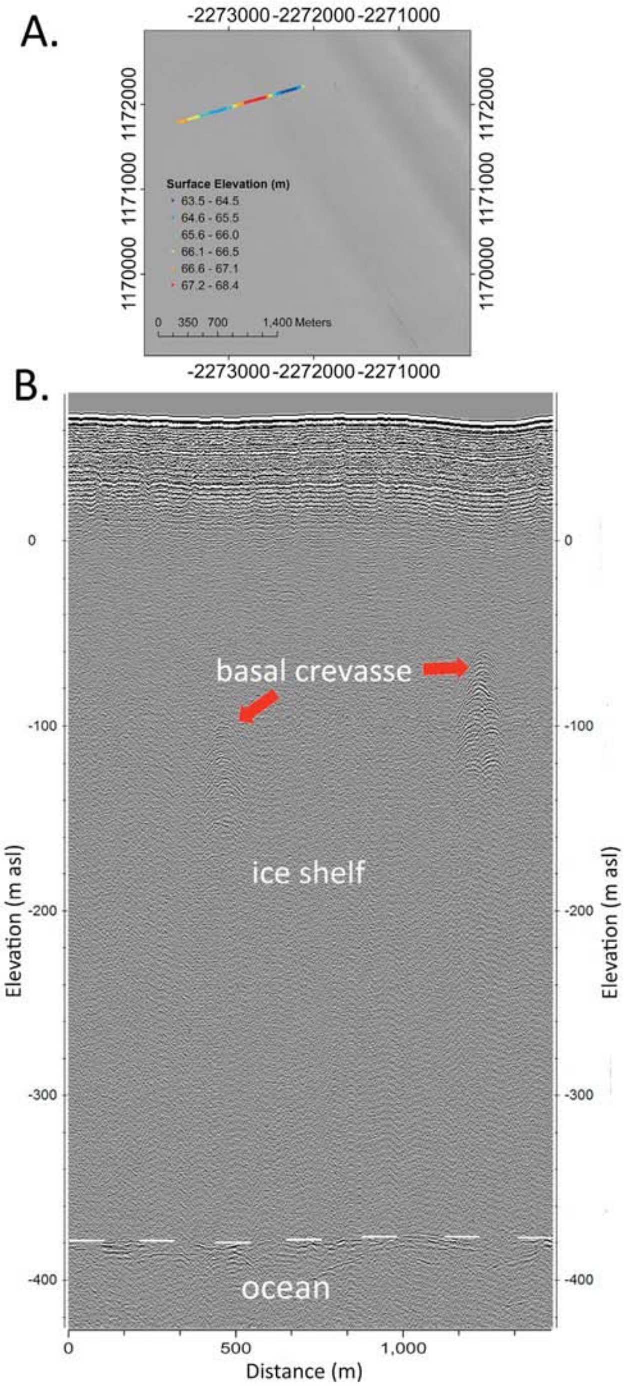

Figure 3. (a) Surface elevations along radar transect (shown in Figure 3b). Note spatial offset between depression in kinematic GPS data and visual imagery due to temporal offset between image and GPS collection. (b) 25 MHz radar profile across basal crevasses (apexes indicated by red arrows). Surface elevations have been corrected to reflect ice shelf topography. Note reduced surface deformation and lack of surface crevassing.

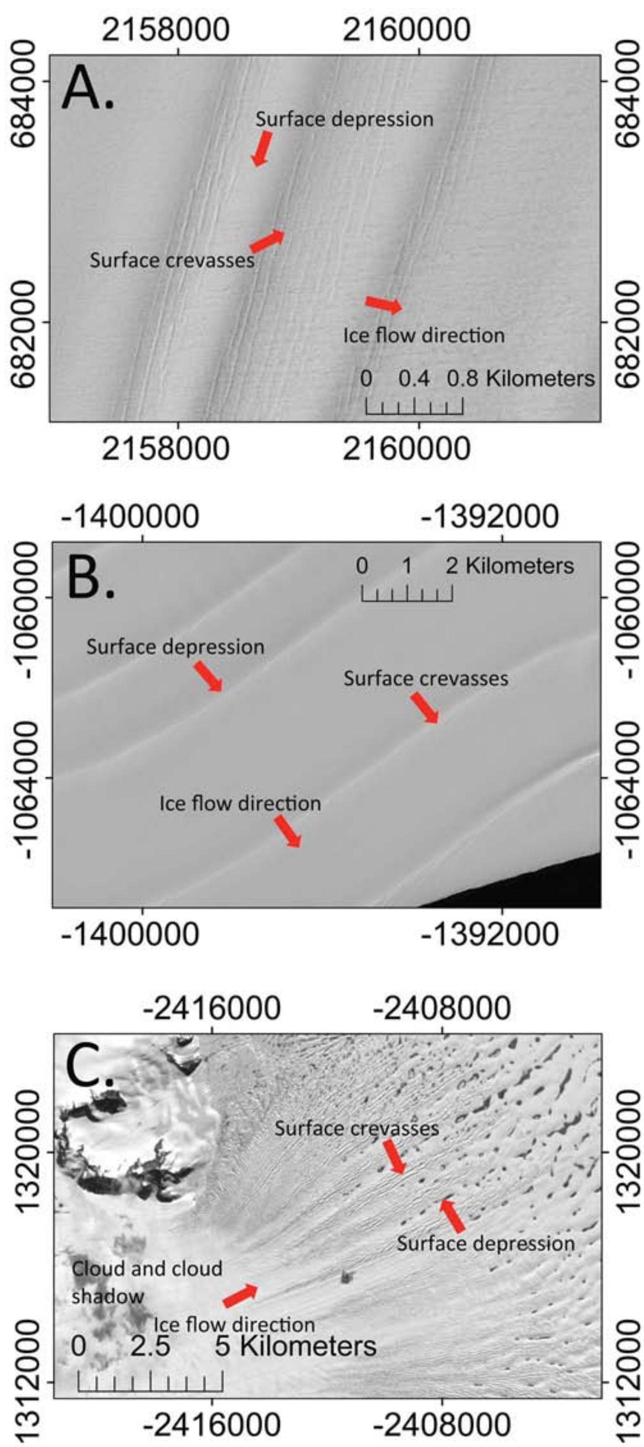

Figure 4. Visible imagery detailing surface depressions, believed to be underlain by basal crevasses, and surface crevassing on the (a) Amery, (b) Getz and (c) former Larsen B Ice Shelves. Locations are indicated in Figure 1a. Imagery in Figures 4a and 4b copyright Digital Globe Inc., 2012.

are aligned parallel to the basal crevasse but on the down sloping flanks of the surface depression, as observed in both the visible imagery (Figure 1b; shadowed features indicated by red arrow) and in the hyperbolic reflections in the upper 10 m of the radargram (Figure 2a; highlighted in red).

[8] We attribute the formation of the surface crevasses to bending stresses induced as the ice shelf surface deforms in order to reach a modified hydrostatic equilibrium [*McGrath et al.*, 2012]. We offer the following observations here to support this hypothesis. We observe two nascent basal crevasses, which are located upstream from the series that extend seaward from Churchill Peninsula, which have propagated to a similar height but with limited surface deformation (1–4 m) and no apparent surface crevassing (Figure 3). Further along flow (i.e. with increased temporal evolution), the basal crevasses have clearly defined surface depressions, down warped firn/ice layers above the basal crevasse and numerous surface crevasses adjacent to the basal crevasse [*McGrath et al.*, 2012]. Together, these observations suggest that the basal crevasse forms first, subsequently followed by surface deformation, the visco-elastic response to the reduced ice thickness above the basal crevasse. However, as this thinner section is partially supported by the full thickness ice to either side, the resulting geometry induces bending stresses, with tension across the crests and down the flanks, sufficient to induce surface crevassing, and compression in the surface depressions, which are free of surface crevasses (Figure 1b).

[9] We now highlight similar surface features, using a combination of Worldview-1 and Landsat imagery, which we interpret, based on their similarity to Larsen C, as the surface expressions of basal crevasses on the Amery, Getz and former Larsen B Ice Shelves. The stress environment causing the basal crevasses to form is different for each ice shelf, yet they all support the notion that basal crevasses can induce surface crevassing and create a surface depression, thereby controlling the location of meltwater ponding. In the eastern section of the Amery Ice Shelf, a series of surface depressions originate in the vicinity of the Gillock Island and extend across-flow by ~40 km (Figure 4a). Numerous surface crevasses (~4–8 per crest; 10–40 m in width) are located on the topographic crests between depressions and aligned parallel with them, whereas the depressions themselves are free of surface crevasses (Figure 4a). Likewise, a series of front parallel, but slightly sinuous surface depressions extend over 20 km near the calving front of the Getz Ice Shelf in the Amundsen Sea sector (Figure 4b). Similarly, ~4–8 surface crevasses, 10–40 m in width are aligned with the basal crevasses, although some extend slightly oblique to the main orientation of the surface depression, which we interpret as being due to a more complex stress environment. Prior to the disintegration of the Larsen B Ice Shelf, the floating outflow of the Hektoria-Green-Evans glacier system had numerous surface crevasses, which had formed *parallel* to flow direction and termed ‘splaying crevasses’ (Figure 4c) [*Glasser and Scambos*, 2008]. The surface crevasses were most abundant on the topographic crests, and were separated by large-scale (10–15 km) linear surface depressions, likely underlain by basal crevasses (Figure 4c). Prior to break-up, discrete meltwater ponds were abundant in the surface depressions, highlighting how such structural features can control meltwater ponding on the shelf surface. Subsequent pond drainage prior to the breakup of Larsen B indicates that a connection was made to the ocean, likely through meltwater-driven crevasse propagation [*Scambos et al.*, 2003]. Both the proximity of this meltwater to widespread surface crevassing and the subsequent iceberg dimensions, which largely overturned during the disintegration event,

suggest that crevasse propagation did occur and that the fracture spacing in this sector was likely governed by the surface crevasse spacing [*Scambos et al.*, 2003].

4. Implications

[10] Meltwater-driven hydrofracture, the process by which water filled surface crevasses fracture downwards, has been suggested to be an important mechanism in the final break up of several ice shelves [*Weertman*, 1973; *van der Veen*, 1998, 2007; *Scambos et al.*, 2000, 2003]. We have shown that basal crevasses, beyond introducing large-scale ice shelf weaknesses, can create both surface depressions and surface crevasses. The most apparent implication of meltwater ponding in the surface depression is if the meltwater were to intersect a flanking surface crevasse, and subsequently establish a channel by which the pond could drain, thereby providing the necessary water volume for continued fracture. Perhaps less obvious, however, is that the increased load in the trough will increase extensional stresses along the flanks and in the vicinity of the basal crevasse apex, potentially leading to further propagation and the possibility for a shear fracture to connect these features [*Bassis and Walker*, 2012]. This structural weakness could be further exploited if hydrofracture originates from the base of the surface trough, where the hydrostatic pressure is the greatest, and where, despite the large-scale compressional environment, incipient surface cracks/fractures are still likely to be present [*Fountain et al.*, 2005]. The presence of the basal crevasse greatly reduces the ice thickness in the vicinity, thereby minimizing the distance through which these small fractures have to propagate prior to creating a full-thickness rift. While the surface crevasses certainly weaken the ice shelf, this latter case highlights the possibility that it is the presence of the basal crevasse that is more important for ice shelf stability. Basal crevasses are an order of magnitude larger in width and depth than the surface crevasses they create, and by concentrating meltwater ponding directly above them, they can control fracture location, and therefore, ice shelf disintegration.

[11] In addition to the observations of melt pond drainage on Larsen B, sediment cores retrieved from beneath both the former Larsen A and Prince Gustav Ice Shelves, record spatially discrete sediment pulses interpreted as the drainage of supraglacial lakes and/or crevasses prior to the ice shelf disintegration event [*Gilbert and Domack*, 2003]. Together, these observations provide clear evidence that fractures do propagate through the ice shelves, although the location where the hydrofracture originated is unclear (i.e. whether it was a proximal surface crevasse or incipient flaw beneath the pond). A corollary can be drawn to supraglacial lake drainage on the Greenland Ice Sheet, where fractures, and later moulins, develop within the lake boundary [*Das et al.*, 2008]. Thus, if hydrofracture does originate from within the pond boundary, the presence of the basal crevasse should make the formation of a full-thickness rift exceedingly efficient.

[12] Previous studies have concluded that the Larsen C Ice Shelf is largely stable and thus not likely to experience a catastrophic collapse at present, despite observations of thinning and flow acceleration in the northerly sector [*Jansen et al.*, 2010; *Khazendar et al.*, 2011]. Basal crevasses have likely been present on the ice shelf for at least the last ~400 years [*McGrath et al.*, 2012], and thus are not likely a reflection of the recent changes in ice shelf thickness or speed, nor suggest that Larsen C is becoming unstable [*Khazendar et al.*, 2011]. In order for basal crevasses to affect the stability of Larsen C, both meltwater production and meltwater ponding would need to increase significantly. At present, only a limited number of melt ponds form each summer, most commonly near the Cabinet Inlet grounding line, likely in response to föhn airflow over the peninsula [*van den Broeke*, 2005]. While melt ponds are spatially limited at present, it is likely that firn densification has significantly contributed to the observed surface lowering over the past three decades [*Holland et al.*, 2011; *Fricker and Padman*, 2012]. If the long-term temperature trends on the AP continue [*Vaughan et al.*, 2003], increased meltwater production and firn densification is likely, in which case, basal crevasses and their surface expressions, including both depressions and crevasses, could have a significant role in future ice shelf disintegration events.

[13] **Acknowledgments.** This work is funded by NSF OPP research grant 0732946. The British Antarctic Survey and field assistant, Tom Weston, provided exceptional field support, without which this work would not have been possible. Geospatial support for this work was supported by the Polar Geospatial Center under NSF OPP agreement ANT-1043681. Careful reviews by Jeremy Bassis and two anonymous reviewers significantly improved the manuscript.

[14] The Editor thanks Doug Benn and Jeremy Bassis for their assistance in evaluating this paper.

References

Bassis, J. N., and C. C. Walker (2012), Upper and lower limits on the stability of calving glaciers from the yield strength envelope of ice, *Proc. R. Soc. A*, *468*, 913–931, doi:10.1098/rspa.2011.0422.

Bindschadler, R., D. G. Vaughan, and P. Vornberger (2011), Variability of basal melt beneath the Pine Island Glacier ice shelf, West Antarctica, *J. Glaciol.*, *57*(204), 581–595, doi:10.3189/002214311797409802.

Burton, J. C., J. M. Amundson, D. S. Abbot, A. Boghosian, L. M. Cathles, S. Correa-Legisos, K. N. Darnell, N. Guttenberg, D. M. Holland, and D. R. MacAyeal (2012), Laboratory investigations of iceberg capsize dynamics, energy dissipation and tsunamigenesis, *J. Geophys. Res.*, *117*, F01007, doi:10.1029/2011JF002055.

Cook, A. J., and D. G. Vaughan (2010), Overview of areal changes of the ice shelves on the Antarctic Peninsula over the past 50 years, *Cryosphere*, *4*, 77–98, doi:10.5194/tc-4-77-2010.

Das, S., I. Joughin, M. D. Behn, I. M. Howat, M. A. King, D. Lizarralde, and M. P. Bhattia (2008), Fracture propagation to the base of the Greenland Ice Sheet during supraglacial lake drainage, *Science*, *320*, 778–781, doi:10.1126/science.1153360.

Doake, C. S. M., H. F. J. Corr, H. Rott, P. Skvarca, and N. W. Young (1998), Breakup and conditions for stability of the northern Larsen Ice Shelf, Antarctica, *Nature*, *391*, 778–780, doi:10.1038/35832.

Förste, C., et al. (2008), The GeoForschungsZentrum Potsdam/Groupe de Recherche de Geodesie Spatiale satellite-only and combined gravity field models: EIGEN-GL04S1 and EIGEN-GL04C, *J. Geod.*, *82*, 331–346, doi:10.1007/s00190-007-0183-8.

Fountain, A. G., R. W. Jacobel, R. Schilchting, and P. Jansson (2005), Fractures as the main pathways of water flow in temperate glaciers, *Nature*, *433*, 618–621, doi:10.1038/nature03296.

Fricker, H. A., and L. Padman (2012), Thirty years of elevation change on Antarctic Peninsula ice shelves from mulitmission satellite radar altimetry, *J. Geophys. Res.*, *117*, C02026, doi:10.1029/2011JC007126.

Gilbert, R., and E. W. Domack (2003), Sedimentary record of disintegrating ice shelves in a warming climate, Antarctic Peninsula, *Geochem. Geophys. Geosyst.*, *4*(4), 1038, doi:10.1029/2002GC000441.

Glasser, N. F., and T. A. Scambos (2008), A structural glaciological analysis of the 2002 Larsen B ice shelf collapse, *J. Glaciol.*, *54*(184), 3–16, doi:10.3189/002214308784409017.

Glasser, N. F., B. Kulessa, A. Luckman, D. Jansen, E. C. King, P. R. Sammonds, T. A. Scambos, and K. C. Jezek (2009), Surface structure and stability of the Larsen C ice shelf, Antarctic Peninsula, *J. Glaciol.*, *55*(191), 400–410, doi:10.3189/002214309788816597.

Guttenberg, N., D. S. Abbot, J. M. Amundson, J. C. Burton, L. Mac Cathles, D. R. MacAyeal, and W. W. Zhang (2011), A computational investigation of iceberg capsize as a driver of explosive ice shelf disintegration, *Ann. Glaciol.*, *52*(59), 51–59, doi:10.3189/172756411799096178.

Haran, T., J. Bohlander, T. Scambos, T. Painter, and M. Fahnestock (2005), MODIS mosaic of Antarctica (MOA) image map, updated 2006, http://nsidc.org/data/nsidc-0280.html, Natl. Snow and Ice Data Cent., Boulder, Colo.

Holland, P. R., H. F. J. Corr, H. D. Pritchard, D. G. Vaughan, R. J. Arthern, A. Jenkins, and M. Tedesco (2011), The air content of Larsen Ice Shelf, *Geophys. Res. Lett.*, *38*, L10503, doi:10.1029/2011GL047245.

Humbert, A., and D. Steinhage (2011), The evolution of the western rift area of the Fimbul Ice Shelf, Antarctica, *Cryosphere*, *5*, 931–944, doi:10.5194/tc-5-931-2011.

Jansen, D., B. Kulessa, P. R. Sammonds, A. Luckman, E. C. King, and N. F. Glasser (2010), Present stability of the Larsen C ice shelf, Antarctic Peninsula, *J. Glaciol.*, *56*(198), 593–600, doi:10.3189/002214310793146223.

Jezek, K. C., C. R. Bentley, and J. W. Clough (1979), Electromagnetic sounding of bottom crevasses on the Ross Ice Shelf, Antarctica, *J. Glaciol.*, *24*(90), 321–330.

Khazendar, A., E. Rignot, and E. Larour (2007), Larsen B Ice Shelf rheology preceding its disintegration inferred by a control method, *Geophys. Res. Lett.*, *34*, L19503, doi:10.1029/2007GL030980.

Khazendar, A., E. Rignot, and E. Larour (2011), Acceleration and spatial rheology of Larsen C Ice Shelf, Antarctic Peninsula, *Geophys. Res. Lett.*, *38*, L09502, doi:10.1029/2011GL046775.

Luckman, A., D. Jansen, B. Kulessa, E. C. King, P. Sammonds, and D. I. Benn (2012), Basal crevasses in Larsen C Ice Shelf and implications for their global abundance, *Cryosphere*, *6*, 113–123, doi:10.5194/tc-6-113-2012.

MacAyeal, D. R., T. A. Scambos, C. Hulbe, and M. Fahnestock (2003), Catastrophic ice-shelf break-up by an ice-shelf-fragment-capsize mechanism, *J. Glaciol.*, *49*(164), 22–36, doi:10.3189/172756503781830863.

McGrath, D., K. Steffen, T. Scambos, H. Rajaram, G. Casassa, and J. L. Rodriguez Lagos (2012), Basal crevasses and associated surface crevassing on the Larsen C ice shelf, Antarctica, and their role in ice-shelf instability, *Ann. Glaciol.*, *58*(60), 10–18, doi:10.3189/2012AoG60A005.

Nicholls, K. W., C. J. Pudsey, and P. Morris (2004), Summertime water masses off the northern Larsen C Ice Shelf, Antarctica, *Geophys. Res. Lett.*, *31*, L09309, doi:10.1029/2004GL019924.

Orheim, O. (1982), Radio echo-sounding of Riiser-Larsenisen, *Ann. Glaciol.*, *3*, 355.

Padman, L., H. A. Fricker, R. Coleman, S. Howard, and L. Erofeeva (2002), A new tide model for the Antarctic ice shelves and seas, *Ann. Glaciol.*, *34*, 247–254, doi:10.3189/172756402781817752.

Rignot, E., G. Casassa, P. Gogineni, W. Krabill, A. Rivera, and R. Thomas (2004), Accelerated discharge from the Antarctic Peninsula following the collapse of Larsen B ice shelf, *Geophys. Res. Lett.*, *31*, L18401, doi:10.1029/2004GL020697.

Rott, H., P. Skvarca, and T. Nagler (1996), Rapid collapse of northern Larsen Ice Shelf, *Antarct. Sci.*, *271*, 788–792.

Scambos, T. A., C. Hulbe, M. Fahnestock, and J. Bohlander (2000), The link between climate warming and break-up of ice shelves in the Antarctic Peninsula, *J. Glaciol.*, *46*, 516–530, doi:10.3189/172756500781833043.

Scambos, T. A., C. Hulbe, and M. Fahnestock (2003), Climate-induced ice shelf disintegration in the Antarctic Peninsula, in *Antarctic Peninsula Climate Variability: Historical and Paleoenvironmental Perspectives*, *Antarct. Res. Ser.*, vol. 79, edited by E. Domack et al., pp. 79–92, AGU, Washington, D. C., doi:10.1029/AR079p0079.

Scambos, T. A., H. A. Fricker, C.-C. Liu, J. Bohlander, J. Fastook, A. Sargent, R. Massom, and A.-M. Wu (2009), Ice shelf disintegration by plate bending and hydro-fracture: Satellite observations and model results of the 2008 Wilkins ice shelf break- ups, *Earth Planet. Sci. Lett.*, *280*, 51–60, doi:10.1016/j.epsl.2008.12.027.

Shabtaie, S., and C. R. Bentley (1982), Tabular icebergs: Implications from geophysical studies of ice shelves, *J. Glaciol.*, *28*(100), 413–430.

Shepherd, A., D. Wingham, T. Payne, and P. Skvarca (2003), Larsen Ice Shelf has progressively thinned, *Science*, *302*(5646), 856–859, doi:10.1126/science.1089768.

Swithinbank, C. (1977), Glaciological research in the Antarctic Peninsula, *Philos. Trans. R. Soc. London, Ser. B*, *279*, 161–183, doi:10.1098/rstb.1977.0080.

van den Broeke, M. (2005), Strong surface melting preceded collapse of Antarctic Peninsula ice shelf, *Geophys. Res. Lett.*, *32*, L12815, doi:10.1029/2005GL023247.

van der Veen, C. J. (1998), Fracture mechanics approach to penetration of surface crevasses on glaciers, *Cold Reg. Sci. Technol.*, *27*, 31–47, doi:10.1016/S0165-232X(97)00022-0.

van der Veen, C. J. (2007), Fracture propagation as means of rapidly transferring surface meltwater to the base of glaciers, *Geophys. Res. Lett.*, *34*, L01501, doi:10.1029/2006GL028385.

Vaughan, D. G. (2006), Recent trends in melting conditions on the Antarctic Peninsula and their implications for ice-sheet mass balance and sea level, *Arct. Antarct. Alp. Res.*, *38*(1), 147–152, doi:10.1657/1523-0430(2006)038[0147:RTIMCO]2.0.CO;2.

Vaughan, D. G., G. J. Marshall, W. M. Connolley, C. Parkinson, R. Mulvaney, D. A. Hodgson, J. C. King, C. J. Pudsey, and J. Turner (2003), Recent rapid regional climate warming on the Antarctic Peninsula, *Clim. Change*, *60*, 243–274, doi:10.1023/A:1026021217991.

Vieli, A., A. J. Payne, A. Shepherd, and Z. Du (2007), Causes of pre-collapse changes of the Larsen B ice shelf: Numerical modelling and assimilation of satellite observations, *Earth Planet. Sci. Lett.*, *259*, 297–306, doi:10.1016/j.epsl.2007.04.050.

Weertman, J. (1973), Can a water-filled crevasse reach the bottom surface of a glacier?, *IAHS Publ.*, *95*, 139–145.